

# Resveratrol loaded glycyrrhizic acid-conjugated human serum albumin nanoparticles for tail vein injection II: pharmacokinetics, tissue distribution and bioavailability

Mingfang Wu<sup>a,b,\*</sup>, Chen Zhong<sup>c,\*</sup>, Yiping Deng<sup>a,b</sup>, Qian Zhang<sup>a,b</sup>, Xiaoxue Zhang<sup>a,b</sup> and Xiuhua Zhao<sup>a,b</sup>

<sup>a</sup>College of Chemistry, Chemical Engineering and Resource Utilization, Northeast Forestry University, Harbin, Heilongjiang, China; <sup>b</sup>Key Laboratory of Forest Plant Ecology, Northeast Forestry University, Ministry of Education, Harbin, Heilongjiang, China; <sup>c</sup>State Key laboratory of Genetic Engineering, School of Life Sciences, Fudan University, Shanghai, China

## ABSTRACT

There are many kinds of biological activities of resveratrol itself, but its clinical application is limited by its poor solubility in water and low bioavailability. Therefore, we have prepared glycyrrhizic acid-conjugated human serum albumin nanoparticles wrapping resveratrol nanoparticles (GL-HSA-RESNPs). The purpose of this study was to investigate the bioavailability, pharmacokinetics and tissue distribution of resveratrol in rats after single-dose tail vein injection administration of GL-HSA-RESNPs. A sensitive and reliable high performance liquid chromatography (HPLC) method was established to verify the content of resveratrol in rat plasma and organs. The  $C_{max}$  value after GL-HSA-RESNPs administration was significantly higher than that of resveratrol suspension ( $933 \pm 76.64$  ng/mL vs.  $618 \pm 42.54$  ng/mL,  $p < .01$ ). The  $T_{max}$  value obtained after GL-HSA-RESNPs administration was significantly shorter than that after resveratrol suspension administration ( $0.17 \pm 0.01$  h vs.  $0.25 \pm 0.01$  h,  $p < .001$ ). The bioavailability of GL-HSA-RESNPs was 4.25 times higher than that of the pure resveratrol. The concentration of resveratrol in the main organs of rats treated with the GL-HSA-RESNPs was higher than that in rats treated with the pure resveratrol. Rats treated with GL-HSA-RESNPs had the highest concentration of resveratrol in their liver. It is indicated that GL-HSA-RESNPs is a promising liver-targeted delivery system that improves the in vivo bioavailability of resveratrol.

## ARTICLE HISTORY

Received 3 November 2019  
Revised 10 December 2019  
Accepted 10 December 2019



## KEYWORDS

Resveratrol; tail vein administration; pharmacokinetics; tissue distribution; HPLC

## 1. Introduction

Resveratrol (3,5,4-trihydroxy-*trans*-stilbene, RES) is a natural polyphenol antioxidant from grapes, *Polygonum cuspidatum* and other plants. (Liang et al., 2013; Zu et al., 2016). It is a type of antibiotic that can resist mold infection when the plant is in a harsh environment or when it is attacked by a pathogen. In these plants, the content of RES in *Polygonum cuspidatum* was relatively high. Studies have shown that RES has a variety of protective effects on human health such as an analgesia (Bazzo et al., 2013), age defying (Hsu et al., 2014), regulation of lipoprotein metabolism, platelet aggregation inhibitor and vasodilator (Wang et al., 2008). In the pancreatic tissues, RES increases antioxidant enzymes such as superoxide dismutase, catalase, glutathione-S-transferase, and glutathione peroxidase to improve the activity of antioxidant defenses and protects pancreatic cells from free radical damage (Szkudelska et al., 2014). Several studies have shown that RES administration increases insulin sensitivity in patients with T2DM and diabetic rats (Zhu et al., 2017). In addition, the most effective role of RES is that it can inhibit the occurrence, promotion, and progression of tumor (Li &

Wei, 2013). RES has been shown to effectively inhibit the proliferation of ovarian cancer cells (SKOV3 and A2780) and inhibit the glycolysis pathway to induce apoptosis (Liu et al., 2018). Although RES has significant effects in terms of anti-oxidation and anti-tumor effects, it is difficult to dissolve in water and has a short half-life in vivo, resulting in poor absorption in vivo, which weakens its therapeutic effect (Ethemoglu et al., 2017). From a transport perspective, RES has the potential for low water solubility and dissolution restriction from the gastrointestinal tract (Singh et al., 2016). At present, in order to overcome this disadvantage, an encapsulation method such as a liposome, a polymer-based nanoparticle, a hydrogel and serum albumin can be used (Han et al., 2011; Li et al., 2013; Jiang et al., 2014; Merino et al., 2015). The use of serum albumin in these methods may be one of the most suitable carrier materials for insoluble anticancer drugs (Aihui et al., 2010). RES can be used in combination with albumin to significantly enhance its water solubility and bioavailability. Nano-size has obvious advantages over other technologies that achieve these goals (Kwok & Chan, 2014; Jain et al., 2015). Nanoemulsion systems can greatly help to resolve their

**CONTACT** Xiuhua Zhao  [xiuhua.zhao@nefu.edu.cn](mailto:xiuhua.zhao@nefu.edu.cn)  College of Chemistry, Chemical Engineering and Resource Utilization, Northeast Forestry University, 26 hexing road, Harbin, Heilongjiang, 150040, China

\*Mingfang Wu and Chen Zhong contributed equally to this work.

© 2019 The Author(s). Published by Informa UK Limited, trading as Taylor & Francis Group.

This is an Open Access article distributed under the terms of the Creative Commons Attribution-NonCommercial License (<http://creativecommons.org/licenses/by-nc/4.0/>), which permits unrestricted non-commercial use, distribution, and reproduction in any medium, provided the original work is properly cited.

potential pharmacokinetic limitations and preserve the therapeutic value of drugs (Musthaba et al., 2010; Sengupta & Chatterjee, 2017).

In recent years, nano-carriers have significant advantages in anticancer drug delivery system (DDSs). It can enhance the high permeability and retention effect of the drug in solid tumor and improve the circulation time in the blood. In addition, multi-functional nano-carriers can endow them with targeting function and improve the selective uptake efficiency of cells (Moros et al., 2013; Wang et al., 2016; Yin et al., 2017; Wang et al., 2018). Human serum albumin (HSA) is a kind of human-derived substance, which has the characteristics of non-toxicity, non-immunogenicity and good biocompatibility (Kratz, 2008). Human serum albumin exists in a large number of human blood, has excellent water solubility and safety, and has been widely used as a multifunctional drug delivery carrier (Deng et al., 2018; Hoonjan et al., 2018). In addition, the functional groups such as carboxyl and amino groups on the surface of albumin are beneficial to the surface functionalization of albumin nanoparticles (Mo et al., 2007; Yu et al., 2014). Drugs that use human serum albumin as a carrier can enhance the dissolution rate and saturation solubility of drugs by intravenous injection. Cumulative data show that when the poorly hydrophilic drug binds to human serum albumin, the bioavailability of the drug can be increased (Kumar et al., 2013; Taneja & Singh, 2017).

Recently, our research team reported the preparation, characterization and liver cancer targeting of glycyrrhizic acid-conjugated human serum albumin loaded RES nanoparticles (GL-HSA-RES-NPs) (Wu et al., 2017). GL-HSA-RES-NPs were prepared by a high-pressure homogeneous emulsification method with an average particle size of  $108.1 \pm 5.3$  nm and a polydispersity index (PDI) of 0.001. In this study, we explored the bioavailability, pharmacokinetics and tissue distribution after intravenous injection of GL-HSA-RES-NPs in rats.

## 2. Materials and methods

### 2.1. Chemicals and reagents

RES (purity 98%) was purchased from Dongming Growth Biotechnology Co., Ltd (Heze, Shandong, China). GL-HSA-RES-NPs were homemade in the laboratory. Phloretin (internal standard) was purchased from the Shanghai Wan Jiang Biotechnology Co., Ltd (Shanghai, China). Acetonitrile and acetic acid were of HPLC grade and methanol was obtained from Sigma-Aldrich (St. Louis, MO, USA). Drug-free blood and tissue were obtained from healthy Sprague–Dawley (SD) rats of both sexes and stored in a  $-20^{\circ}\text{C}$  refrigerator. The experimental water was obtained from ULUPURE-H water purification system (Zhengzhou Youerpu instrument and equipment Co., Ltd., Henan, China). GL-HSA-RES-NPs were prepared and characterized in this laboratory.

### 2.2. Preparation of GL-HSA-RES-NPs

GL-HSA-RES-NPs was obtained by the high-pressure homogeneous emulsification method (Wu et al., 2017). Briefly, the

glycyrrhizic acid (GL) of 59.6 mg was added to the methanol solution of 4.0 mL and treated in ultrasonic bath for 30 s (Li et al., 2005). The suspension was slowly dripped into NaIO<sub>4</sub> solution (4.0 mL) and stirred for 1 h. The HSA of 50 mg was dissolved in the carbonate buffer (pH = 9.6) of 14 mL and fully mixed with the previous suspension. The pH of the mixed solution was adjusted to 10.0 and stirred fully for 6 h at room temperature. GL-HSA solution was dialyzed in deionized water for 3 days and freeze-dried to obtain GL-HSA freeze-dried powder. RES was fully dissolved in a mixed solution containing chloroform and methanol (volume ratio 7:3). The suspension was slowly dripped into the deionized water containing GL-HSA, accompanied by high-speed homogeneous stirring. The residual organic solvent was removed by rotary evaporation system at  $45^{\circ}\text{C}$  to obtain GL-HSA-RES-NPS suspension. At last, GL-HSA-RES-NPs particles were obtained by freeze drying. There was no significant difference in morphology, average particle size and potential parameters of GL-HSA-RES-NPs after freeze drying. GL-HSA-RES-NPs freeze-dried powder was suspended in deionized water and injected intravenously into the tail of rats.

### 2.3. Animals

SD rats were purchased from Beijing Vital River Laboratory Animal Technology Co., Ltd., (Beijing, China) weighing between 190 g and 220 g. The feeding environment of SD rats was  $25^{\circ}\text{C}$ , the relative humidity was 60% and provided an appropriate period of diurnal light variation (12 h of light and 12 h of darkness). SD rats were fed for a week before the experiment, free to eat (without soy protein) and drinking water. All SD rats fasted on the eve of the experiment. All animal experiments were implemented in accordance with the Guidelines for the Care of Northeast Forestry University. Animal experiments were approved by the Ethics Committee of the Northeast Forestry University (approval No. 2019–0513/1).

### 2.4. Animal experiments and sampling

A total of 12 rats (6 males and 6 females) were assigned to two groups: GL-HSA-RES-NPs group and raw RES group. Animals in the former group were administered a single tail vein injection dose of lyophilizing GL-HSA-RES-NPs powder suspended in water (equivalent to 6 mg/kg of RES). Those in the latter group were given 6 mg/kg of free RES sufficiently dissolved in 5% (v/v) DMSO and 20% (w/v) PEG-400 in 5% (v/v) glucose solution. 0.3 mL blood was taken from orbital venous plexus at different time points (5, 15, and 30 min, and at 1, 2, 4, 8, 12, and 24 h) and transferred to heparinized test tube. The plasma was obtained by 6000 r/min centrifugation 10 min and stored at  $-20^{\circ}\text{C}$ .

For the study of tissue distribution, 72 rats (36 males and 36 females) received the same administered dose in the above description. 6 rats of each preparation were sacrificed at 0.25, 0.5, 1, 2, 4, and 6 h after administration. Heart, liver, spleen, lung, kidney, and brain tissue samples were obtained from each rat. All tissue samples were washed twice with

sterile saline to absorb excess water and immediately stored in a  $-20^{\circ}\text{C}$  freezer until later analysis.

To study the excretion of RES after tail vein administration in rats, 12 rats (6 males and 6 females) were divided into two groups: GL-HSA-RES-NPs group and raw RES group with same dosing as described above. The rats were placed independently in urine and fecal metabolic cages to collect all urine and feces from each drug sample. Quantitative collection of urine and feces within 24 h. Measure and record the volume of urine and the weight of feces, and store the sample at  $-20^{\circ}\text{C}$ .

## 2.5. Toxicity experiment

36 SD rats weighing  $190 \pm 20$  g were randomly divided into control group ( $n = 12$ ), pure RES group ( $n = 12$ ) and GL-HSA-RESNPs group ( $n = 12$ ). The experimental group was treated with RES 6 mg/kg daily for 2 weeks. The control group was given normal saline through caudal vein every day. During this time, all rats were free to drink water and diet. Two weeks later, the rats were sacrificed to obtain various tissues from the rats (heart, liver, spleen, lungs, and kidneys) for weighing (accurate to 0.01). The index of immune organs was calculated according to the following formula:

$$\begin{aligned} & \text{Immune organ index} \\ & = \text{Weight of immune organs (g)} / \text{Body Weigh (g)} \quad (1) \end{aligned}$$

## 2.6. Plasma sample treatment

For the extraction of RES from rat plasma,  $10 \mu\text{L}$  of phloretin solution was added to  $200 \mu\text{L}$  of rat plasma. Next,  $400 \mu\text{L}$  of methanol solution was added to the above suspension to precipitate protein, and the sample was vortexed for 5 min and centrifuge at  $10,000 \text{ r/min}$  for 10 min. The supernatant sample evaporates to dry under  $\text{N}_2$  flow. The residue is fully dissolved by adding  $200 \mu\text{L}$  methanol to the residue and placing it in the ultrasonic oscillator. The suspension was centrifuged at a speed of  $10,000 \text{ r/min}$  for 5 min, and  $10 \mu\text{L}$  of the supernatant was absorbed and detected by HPLC.

## 2.7. Tissue sample treatment

Thaw each chilled tissue sample at room temperature and  $0.2 \text{ g}$  of the samples were cut into small pieces were placed in a glass homogenizer.  $400 \mu\text{L}$  saline was added to each tissue sample and homogenized by using an electric high-speed homogenizer. Calibration standards and quality control samples for RES analysis were prepared by adding known amounts of RES to normal tissues, which were homogenized in the same manner as described above. Accurately absorb  $100 \mu\text{L}$  of homogenate and place it in a stoppered centrifuge tube, add  $10 \mu\text{L}$  of internal standard and  $400 \mu\text{L}$  of methanol, vortex and mix for 10 min, centrifuge at  $10,000 \text{ r/min}$  for 10 min, and blow dry with nitrogen. The dried residue was then reconstituted in  $100 \mu\text{L}$  methanol. After being ultrasonicated for 5 min and the suspension was centrifuged at  $10,000 \text{ r/min}$  for 5 min. The supernatant of  $10 \mu\text{L}$  was

accurately absorbed and injected into HPLC system for detection. The concentration of RES in intact tissue was calculated according to the concentration of RES in  $0.2 \text{ g}$  tissue. Blank samples of all matrices were also extracted to ensure the absence of endogenous interfering peaks.

## 2.8. Preparation of standard solution

### 2.8.1. Preparation of RES standard reserve solution

The precision weighing RES standard  $1 \text{ mg}$  was placed in a  $50 \text{ mL}$  brown volumetric bottle. The ultrasonic treatment of methanol solution was added to dissolve it completely and fix the volume to the calibration line. The RES standard reserve solution of  $0.02 \text{ mg/mL}$  was preserved away from light at  $4^{\circ}\text{C}$ .

### 2.8.2. Preparation of internal standard solution

The phloretin standard for precision weighing  $2 \text{ mg}$  was placed in a  $50 \text{ mL}$  brown volumetric bottle. The mother liquor of  $0.04 \text{ mg/mL}$  was obtained by adding methanol solution to dissolve it completely and fix its volume to the calibration line. The mother liquid of  $5 \text{ mL}$  was accurately taken and placed in a  $50 \text{ mL}$  brown volume flask. Methanol solution was added to it to fix the volume to the calibration line. Finally, an internal standard solution with a mass concentration of  $4 \mu\text{g/mL}$  was obtained and stored in a refrigerator at  $4^{\circ}\text{C}$ .

### 2.8.3. Preparation of RES series standard solution

A certain amount of RES standard solution was precisely absorbed and gradually diluted with methanol into  $0.4, 1, 2, 4, 10, 16,$  and  $20 \mu\text{g/mL}$  RES standard solution.  $10 \mu\text{L}$  of standard solution and  $10 \mu\text{L}$  of internal standard solution were absorbed and added to  $200 \mu\text{L}$  plasma. According to the treatment method described in Section 2.6, the final series of standard solution concentrations are  $20, 50, 100, 200, 500, 800,$  and  $1000 \text{ ng/mL}$ .  $10 \mu\text{L}$  of supernatant was taken into HPLC system for analysis and detection.

## 2.9. Apparatus and HPLC conditions

HPLC method was realization of HPLC method by Agilent chromatograph. The chromatographic column:  $\text{C}_{18}$  reverse-phase column ( $250 \text{ mm} \times 4.6 \text{ mm}, 5 \mu\text{m}$ , China);  $\text{C}_{18}$  guard column ( $10 \text{ mm} \times 4.6 \text{ mm}$ , China); The mobile phase:  $30:70$  (v/v) mixtures of acetonitrile and  $0.2\%$  acetic acid solution; the column temperature:  $25^{\circ}\text{C}$ ; the flow rate:  $1.0 \text{ mL/min}$ ; the detection wavelength:  $306 \text{ nm}$ ; the injection volume:  $10 \mu\text{L}$ .

## 2.10. Analytical method validation

The stability, specificity, linearity, recovery, accuracy, and precision of the samples are measured in accordance with the bioanalytical method validation guidance for industry.

### 2.10.1. Selectivity and specificity

The purpose of selective and specific detection is to eliminate interference from endogenous substances in plasma samples. This method is established by comparing blank plasma from different sources (containing standard and internal standards).

### 2.10.2. Extraction recovery

The RES peak area acquired from plasma or tissue samples was determined by HPLC to be A. Adding an equal amount of RES standard solution to methanol and obtaining a peak area by HPLC was B. The recovery was determined by the ratio of A to B. Three different concentrations of RES were detected in plasma (20, 500, and 1000 ng/mL) and tissue (50, 1000, and 2000 ng/g).

The linearity of the standard curve reflects the relationship between the measured drug concentration and the instrument response value. Generally, the regression equation obtained by regression analysis method is used to evaluate it. Linear equations were tested at 7 concentration levels with a coverage of 20–1000 ng/mL (20, 50, 100, 200, 500, 800, and 1000 ng/mL) in plasma and 40–2000 ng/g (40, 100, 200, 400, 800, 1600, and 2000 ng/g) in tissue samples. The calibration curve was established by plotting the relationship between the peak area ratio of RES to internal standard and the concentration of RES. The parameters of intercept, slope and correlation coefficient are obtained by least square regression equation.

Blank rat plasma containing 20, 500, and 1000 ng/mL and blank tissue samples containing 50, 1000, and 2000 ng/g were prepared. 6 sample analyses were performed for each mass concentration for 3 days for analysis accuracy and precision. The mass concentration of RES in the sample was calculated from the standard curve of the day, and compared with the actual formulated mass concentration to determine the accuracy of the method. The relative standard deviation (RSD) was used to evaluate intra-day and inter-day precision.

The concentration of the calibration standard back should generally be within  $\pm 15\%$  of the indicated value, and the lower limit of quantitation (LLOQ) should be within  $\pm 20\%$ . The LLOQ measured at each concentration level should not exceed 20% of the coefficient of variation CV and the RSD should not exceed 15% of the CV.

Blank rat plasma containing 20, 500, and 1000 ng/mL and blank tissue samples containing 50, 1000, and 2000 ng/g were prepared and tested for stability under various conditions, including: the sample was stored at 20 °C for 24 h; after three repeated freeze-thaw cycles (–20 °C to room temperature); store frozen at –20 °C for 30 days; store at 4 °C for 24 h. When the obtained standard deviation of the concentration is within the range of  $\pm 15\%$ , the compound is considered to be stable.

### 2.11. Pharmacokinetic data analysis

This experiment uses DAS2.0 software (Shanghai, China) to model the data. The pharmacokinetic studies in vivo after tail vein injection of GL-HSA-RES-NPs and the raw RES in rats met a three-compartment model with a weight factor of 1.

### 2.12. Excreta sample treatment and analysis

0.1 g of each fecal sample was thawed and then homogenized by adding 1 mL of methanol. Samples were centrifuged at 10,000 rpm for 5 min. The supernatant was blown dry with nitrogen. The residue was redissolved in 200  $\mu$ L of mobile phase solution and vortex mixed for 5 min and centrifuged at 13,000 rpm for 10 min. Take the supernatant 10  $\mu$ L into the HPLC analysis.

After each urine thawed, 100  $\mu$ L each was added to 200  $\mu$ L of methanol and ultrasonic for 5 min and then centrifuged (10,000 rpm) for 3 min. Supernatant was immediately analyzed by HPLC.

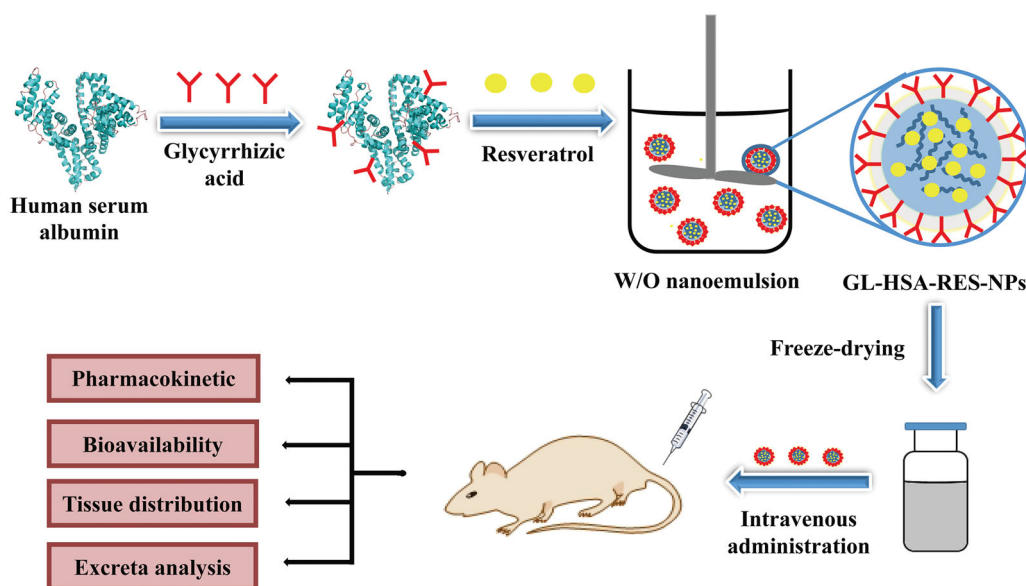
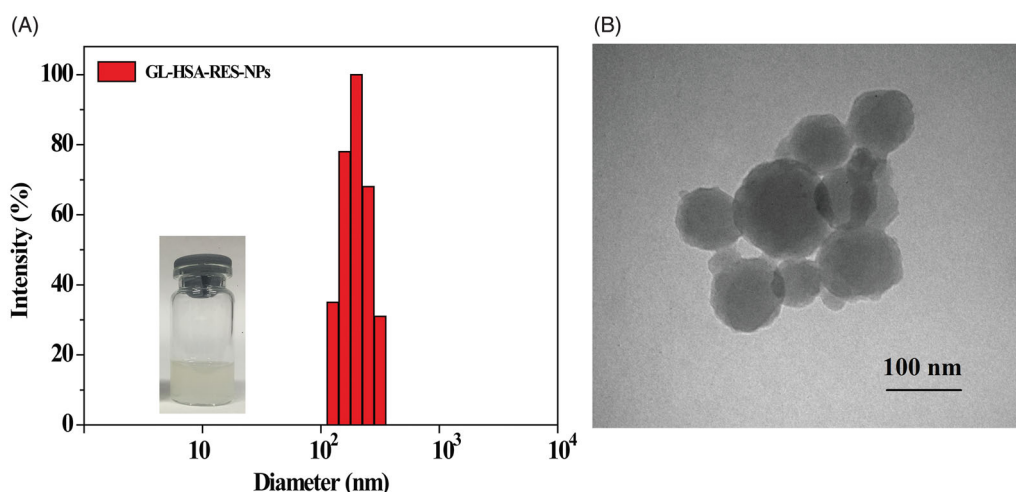
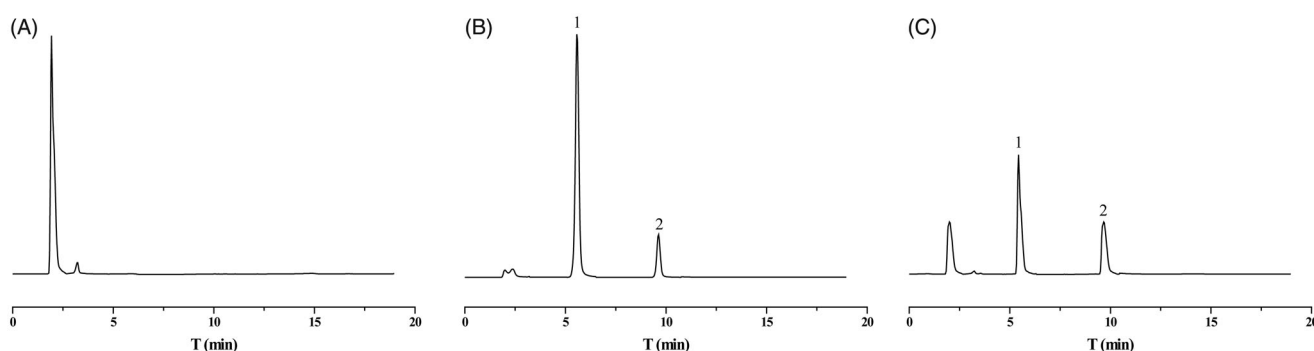


Figure 1. The schematic diagram of the preparation process of GL-HSA-RES-NPs.





**Figure 2.** DLS size distribution (A) and TEM images (B) of GL-HSA-RES-NPs.



**Figure 3.** High performance liquid chromatogram of RES and internal standard in rat plasma. (A) Chromatograms of blank plasma; (B) blank plasma containing RES and internal standard; (C) rat plasma was taken 1 h after a single tail vein injection of GL-HSA-RES-NPs (contains 6 mg/kg RES). Peak 1: RES (retention time = 5.5 min); Peak 2: phloretin (retention time = 9.7 min).

### 2.13. Statistical analysis

The results of statistical analysis are obtained by using SPSS software. The measurements were repeated at least three times and the results showed an average of  $\pm$ SD. The one-way analysis of variance (ANOVA) method was used in data analysis. A  $p$ -value  $< .05$  or  $.01$  was considered statistically significant.

## 3. Results and discussion

### 3.1. Characterizations

In this study, GL-HSA-RES-NPs suspension was prepared by high pressure homogeneous emulsification (Figure 1). Taking the particle size as the evaluation standard, the optimum preparation conditions were obtained by single factor experiment and orthogonal experiment ( $C_{\text{HSA}} = 4 \text{ mg/mL}$ ,  $V_{\text{inorganic}}:V_{\text{organic}}=9:1$ , homogenate speed = 8000 r/min, homogenate time = 5 min, homogenization pressure = 800 bar and homogenization frequency = 9). The average particle size of GL-HSA-RES-NPs obtained under the optimum conditions was  $108.1 \pm 5.3 \text{ nm}$ . The high pressure homogeneous emulsification method is an effective method, which can keep the precipitated small particles and produce smaller particles than the traditional methods. It is observed by

**Table 1.** RES recovery in rat plasma and tissue samples (data mean  $\pm$  SD,  $n = 3$ ).

Samples	Low concentration (%)	Medium concentration (%)	High concentration (%)
Plasma	$100.53 \pm 4.78$	$97.56 \pm 7.43$	$99.36 \pm 6.45$
Heart	$88.76 \pm 7.46$	$94.65 \pm 5.34$	$91.75 \pm 3.55$
Liver	$86.76 \pm 3.79$	$92.36 \pm 6.86$	$90.43 \pm 5.85$
Spleen	$85.05 \pm 5.67$	$90.82 \pm 5.74$	$89.54 \pm 4.73$
Lung	$87.58 \pm 6.56$	$87.52 \pm 7.54$	$92.65 \pm 2.75$
Kidney	$91.34 \pm 4.87$	$88.64 \pm 3.64$	$94.63 \pm 3.86$
Brain	$83.68 \pm 3.98$	$91.35 \pm 2.76$	$88.17 \pm 7.83$

transmission electron microscope that GL-HSA-RESNPs is uniformly dispersed and spherical (Figure 2). The glycyrrhizic acid coupling amount, drug loading efficiency, drug encapsulation efficiency and zeta potential of GL-HSA-RESNPs were  $112.56 \mu\text{g/mg}$ , 11.5%, 83.6% and  $-21.16 \pm 0.58 \text{ mV}$ , respectively. Besides, drug release studies under PBS (0.15 M, pH 7.4) in vitro showed that GL-HSA-RESNPs delivery system could release slowly and continuously. The original RES exhibited a fast release characteristic, and the release rate of the original RES reached about 58.7% in the first 5 h. The cumulative release of the raw RES was 82.6% after 24 h. However, GL-HSA-RESNPs showed a very stable pattern of continuous release. The cumulative release rate of GL-HSA-RESNPs reached 72.4% after 24 h. These results indicate that GL-HSA-RESNPs significantly affected the sustained drug release.

After the preparation process, fresh GL-HSA-RESNPs was rapidly transformed into solid form by freeze-drying, in order to achieve the follow-up study of pharmacokinetics.

### 3.2. Method validation

Plasma samples obtained from blank plasma and 1 h after tail vein administration of GL-HSA-RES-NPs (contains 6 mg/kg RES) were detected by HPLC. The results obtained are shown in Figure 3. Blank plasma endogenous substances did not interfere with RES and internal standard determination. RES retention time was 5.5 min, retention time of internal standard 9.7 min. The chromatographic separation is good and the method has a high specificity. Low, medium and high amounts of RES are added to the plasma or tissue samples to determine that the relative recovery was acceptable (Table 1). Table 2 shows the results of the standard equation of linear regression. The correlation coefficient of calibration curve obtained by each sample is more than 0.99. The results of accuracy and precision are shown in Table 3, indicating that this method was reliable and repeatable. Table 4 shows the results of the stability of RES. The stability results indicated that the concentration of RES in plasma was unchanged at  $-20^{\circ}\text{C}$  for 60 days. The prepared sample was stable at  $20^{\circ}\text{C}$  for 24 h, and there was no change in rat plasma RES after three freeze-thaw cycles. RES was stably stored in post-preparation samples saved at  $4^{\circ}\text{C}$  for 24 h.

**Table 2.** Calibration curve of RES after adding internal standard.

Samples	Typical equations	$R^2$	Concentration range	LLOQ (n = 3)
Plasma	$y = 0.9653x + 0.0365$	0.9997	20–1000 ng/mL	$0.97 \pm 0.094$
Heart	$y = 0.6477x + 0.0456$	0.9987	40–2000 ng/g	$1.03 \pm 0.096$
Liver	$y = 0.4626x + 0.0489$	0.9992	40–2000 ng/g	$1.12 \pm 0.123$
Spleen	$y = 0.5825x + 0.0647$	0.9993	40–2000 ng/g	$1.07 \pm 0.098$
Lung	$y = 0.6873x + 0.0349$	0.9974	40–2000 ng/g	$1.17 \pm 0.116$
Kidney	$y = 0.6986x + 0.0764$	0.9991	40–2000 ng/g	$1.05 \pm 0.127$
Brain	$y = 0.7357x + 0.0368$	0.9994	40–2000 ng/g	$1.18 \pm 0.113$

**Table 3.** Analytical accuracy and precision of RES in samples.

Analyte	Added concentration	Intra-day (n = 6), Accuracy (%)	Precision (RSD, %)	Inter-day (n = 6), Accuracy (%)	Precision (RSD, %)
Plasma (ng/mL)	20	99.34	4.67	95.37	4.68
	500	98.46	6.28	97.64	7.65
	1000	93.25	9.86	98.75	7.36
Heart (ng/g)	50	101.54	6.36	101.24	4.85
	1000	105.46	4.97	96.49	8.67
	2000	99.27	8.36	103.34	5.76
Liver (ng/g)	50	106.63	9.27	96.82	10.64
	1000	102.74	4.63	94.26	7.35
	2000	101.39	7.68	98.25	6.43
Spleen (ng/g)	50	97.37	10.85	99.45	9.63
	1000	98.47	7.35	95.41	3.76
	2000	109.27	5.75	98.58	7.75
Lung (ng/g)	50	98.73	6.39	102.46	8.36
	1000	96.58	11.37	103.27	5.86
	2000	95.93	9.72	95.24	7.32
Kidney (ng/g)	50	104.88	4.27	102.47	9.53
	1000	102.57	8.19	104.12	6.32
	2000	96.64	3.67	99.45	4.86
Brain (ng/g)	50	96.49	6.85	95.75	10.75
	1000	104.53	9.38	96.26	7.48
	2000	103.37	8.64	97.54	5.74

### 3.3. Pharmacokinetic analysis and bioavailability

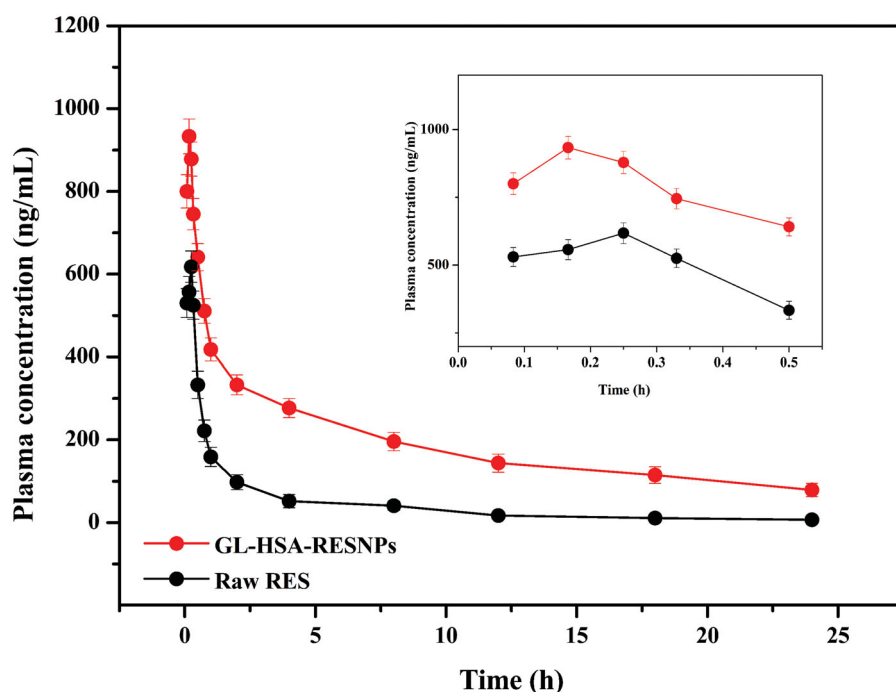
The above verified HPLC method was applied to the pharmacokinetics of RES in rat plasma. Plasma samples were obtained by intravenous injection of GL-HSA-RESNPs and pure RES into the tail of rats. A single dose 24-h pharmacokinetic study was performed in vivo in rats. The mean plasma concentration-time curves for the GL-HSA-RESNPs and raw RES are shown in Figure 4. The pharmacokinetic parameters of RES shown in Table 5 were determined by using the non-atrioventricular model method. Figure 4 shows the results of bioavailability tests for the two sample groups. The results showed that the concentration of RES in the plasma of rats treated with GL-HSA-RESNPs was consistently higher than that of rats treated with the same dose of raw RES. The RES concentrations of the rats treated with GL-HSA-RESNPs and those treated with raw RES reached maximum levels of  $933 \pm 76.64$  ng/mL and  $618 \pm 42.54$  ng/mL ( $p < .01$ ) after  $0.17 \pm 0.01$  h and  $0.25 \pm 0.01$  h ( $p < .001$ ) of drug intake, respectively. The  $C_{\max}$  value of RES in the GL-HSA-RESNPs was significantly higher than that obtained with raw RES. The  $T_{\max}$  of rats treated with GL-HSA-RESNPs was significantly shorter than that of rats treated with the original RES. The  $AUC_{0 \rightarrow t}$  values of RES after GL-HSA-RESNPs and raw RES administration were  $4.67 \pm 0.53$  mg/L·h and  $1.10 \pm 0.25$  mg/L·h ( $p < .001$ ) respectively. The experimental results show that the AUC value of GL-HSA-RESNPs was 4.25 times higher than that of the raw RES. GL-HSA-RESNPs have prolonged the half-life ( $t_{1/2}$ ) and the mean residence time (MRT) in the blood compared with the original RES, while CL<sub>z</sub> and V<sub>z</sub> were decreased with GL-HSA-RESNPs.

### 3.4. Tissue distribution studies

The average concentration-time curve of each tissue after administration of GL-HSA-RESNPs and raw RES by tail vein injection in rats is shown in Figure 5. In the rats treated with the GL-HSA-RESNPs through the tail vein, the  $C_{\max}$  in the six

**Table 4.** Stability of RES in blood and tissue samples.

Analyte	Added concentration	Long-term (-20°C), Re (%)	Short-term (20°C), Re (%)	Freeze-thaw, Re (%)	Post-preparation (20°C), Re (%)
Plasma (ng/mL)	20	-3.56	-4.66	-3.46	-6.45
	500	-2.67	-6.35	-3.56	-1.45
	1000	-4.26	-5.45	-8.35	-2.66
Heart (ng/g)	50	-2.36	-1.45	-11.36	-1.45
	1000	-1.37	-6.35	-2.45	-3.67
	2000	-4.75	-5.83	-6.37	-4.35
Liver (ng/g)	50	-6.35	-9.34	-7.36	-5.36
	1000	-8.36	-3.53	-2.17	-7.35
	2000	-2.74	-10.65	-5.34	-6.72
Spleen (ng/g)	50	-3.54	-6.34	-2.57	-3.62
	1000	-6.37	-2.46	-2.56	-0.46
	2000	-6.26	-0.64	-4.76	-7.75
Lung (ng/g)	50	-4.74	-4.75	-6.34	-0.36
	1000	-8.45	-3.69	-4.76	-2.57
	2000	-7.26	-2.58	-5.34	-2.68
Kidney (ng/g)	50	-2.47	-2.57	-6.55	-3.76
	1000	-4.78	-8.36	-3.57	-6.36
	2000	-8.46	-6.36	-7.45	-5.34
Brain (ng/g)	50	-9.47	-3.54	-7.64	-3.71
	1000	-2.45	-2.65	-7.35	-7.49
	2000	-1.45	-3.57	-3.45	-2.75

**Figure 4.** Mean plasma concentration-time curve of RES after single-dose rat tail vein injection of GL-HSA-RESNPs or raw RES (equivalent to 6 mg/kg RES).

organs collected appeared at 0.5 h after the treatment. In the rats treated with the RES suspension through the tail vein,  $C_{max}$  appeared in the heart, liver, spleen, lungs, and kidneys 1 h after the treatment, and the  $T_{max}$  in the brain was prolonged to 2 h. The  $C_{max}$  values of all organs in GL-HSA-RESNPs group were higher than those in RES suspension group. The  $C_{max}$  values of the various organs in the GL-HSA-RESNPs group were 1.54 times (heart), 2.18 times (liver), 1.46 times (spleen), 1.59 times (lung), 1.19 times (kidney), 2.81 times (brain) of the  $C_{max}$  values of the rats in the RES suspension group, respectively. The  $AUC_{0-6h}$  values obtained by GL-HSA-RESNPs (contains 6 mg/kg RES) in each organ after tail vein injection were liver > heart > spleen > kidney > lung > brain. The  $AUC_{0-6h}$  values obtained by injecting the

**Table 5.** Pharmacokinetic parameters of RES after tail vein administration in rats (data mean  $\pm$  SD,  $n = 6$ ).

Pharmacokinetic parameters	GL-HSA-RES-NPs	Resveratrol suspension
$AUC_{0-t}$ (mg/L·h)	$4.67 \pm 0.53$	$1.10 \pm 0.25$
$AUC_{0-\infty}$ (mg/L·h)	$5.92 \pm 0.61$	$1.19 \pm 0.26$
$C_{max}$ (ng/mL)	$933 \pm 76.64$	$618 \pm 42.54$
$T_{max}$ (h)	$0.17 \pm 0.01$	$0.25 \pm 0.01$
$t_{1/2}$ (h)	$11.05 \pm 2.24$	$9.37 \pm 2.14$
MRT (h)	$8.11 \pm 1.53$	$4.69 \pm 0.067$
CLz (L/h/kg)	$1.01 \pm 0.23$	$5.02 \pm 0.58$
$V_z$ (L/kg)	$16.14 \pm 2.46$	$67.86 \pm 11.23$

$AUC_{0-t}$ : The area under the blood concentration time curve from 0 to the last selected time point;  $AUC_{0-\infty}$ : The area under the blood concentration time curve during the period from 0 to infinity;  $C_{max}$ : Maximum plasma concentration of resveratrol after administration;  $T_{max}$ : is the time when  $C_{max}$  appears;  $t_{1/2}$ : elimination half-life; MRT: mean residence time; CLz: total clearance;  $V_z$ : volume of distribution at terminal state.

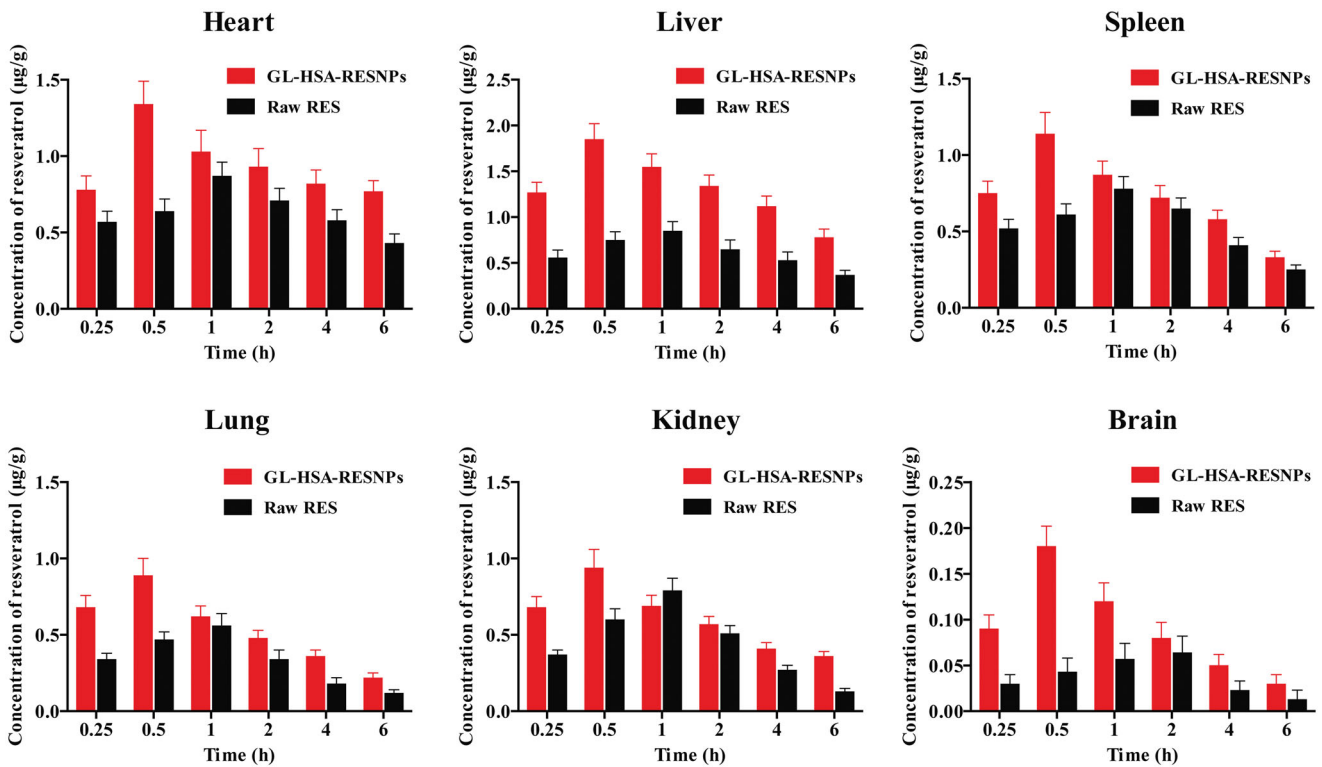


Figure 5. Mean ( $\pm$ SD) plasma concentration-time curve of RES in various organs of rats after administration of GL-HSA-RESNPs and pure RES.

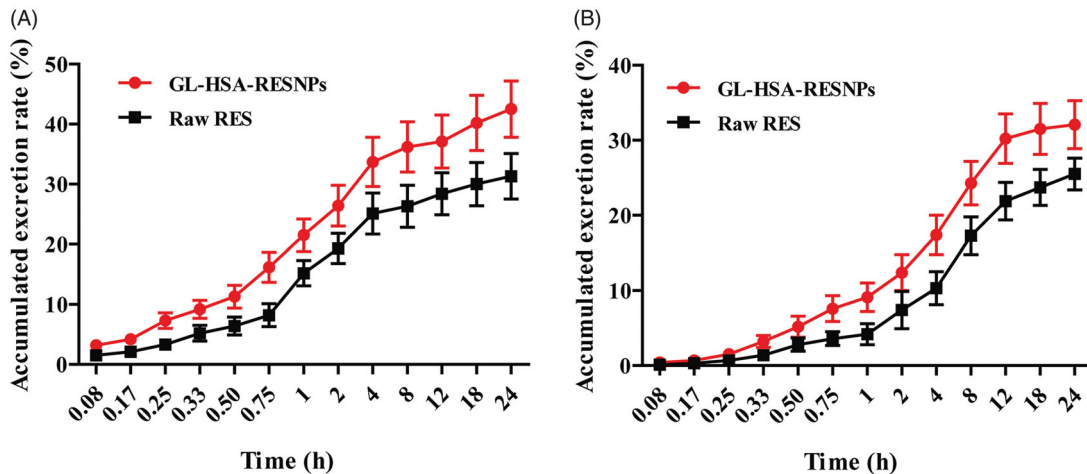


Figure 6. Urinary (A) and fecal (B) cumulative excretion of RES in rats following administration at a single dose of GL-HSA-RESNPs or raw RES.

same amount of pure RES into the tail vein of rats were as follows: heart > liver > spleen > kidney > lung > brain. The ratios of GL-HSA-RES-NPs and pure RES samples in the heart, liver, spleen, lung, kidney, and brain of rats were 1.44, 2.09, 1.30, 1.60, 1.33, and 1.97.

### 3.5. Urinary and fecal excretion

The excretion of GL-HSA-RESNPs and raw RES in urine and feces was illustrated in Figure 6. The total excretion of RES in urine after 24 h of tail administration of GL-HSA-RESNPs or raw RES rats was  $42.52 \pm 4.71\%$  and  $31.32 \pm 3.85\%$  of the administered dose, respectively ( $p < .05$ ). The total excretion of RES in feces within 24 h was  $32.15 \pm 3.23\%$  and

$25.54 \pm 2.16\%$  of the GL-HSA-RESNPs and raw RES, respectively ( $p < .05$ ). The percentage of RES in the urine excreted by the mice within 4 h after injection of the GL-HSA-RESNPs or raw RES in mice was higher, accounting for 79.26% and 80.14% of total urine excretion, respectively. The excretion of RES in the urine within 4–24 h after administration of the GL-HSA-RESNPs and raw RES in the tail vein of mice accounted for 20.74% and 19.86% of total urine excretion, respectively.

### 3.6. Toxicity testing

The results of Table 6 were immune organ index and weight gain of the three groups of rats. The weight gain of rats in GL-HSA-RESNPs group, original RES and control group were



**Table 6.** Effects of GL-HSA-RESNPs on the indices of rat immune organs.

Group	Weight gain (g)	Heart organ index (mg/g)	Liver organ index (mg/g)	Spleen organ index (mg/g)	Lung organ index (mg/g)	Renal organ index (mg/g)
Control group	24.56 ± 3.17	3.35 ± 0.15	48.13 ± 2.16	2.31 ± 0.13	5.57 ± 0.55	8.11 ± 0.30
Raw RES group	36.86 ± 3.46	3.45 ± 0.14	48.87 ± 2.17	2.49 ± 0.14	5.61 ± 0.54	8.15 ± 0.30
GL-HSA-RESNPs group	34.25 ± 3.36	3.39 ± 0.14	48.65 ± 2.15	2.38 ± 0.13	5.63 ± 0.53	8.13 ± 0.31

34.25 ± 3.36 g, 36.86 ± 3.46 g and 24.56 ± 3.17 g, respectively. The above results showed that the weight gain of rats in the experimental group was higher than that in the control group. Therefore, it is suggested that the original RES and GL-HSA-RESNPs have a slight effect on the body weight of rats, but have no toxic effect on their organs. In addition, there was no significant difference in the immune organ index between the control group and the experimental group.

#### 4. Conclusion

As far as I know, the pharmacokinetics and tissue distribution of RES albumin nanoparticles in rats have not been reported before. In this study, a new and reliable HPLC method was established for the determination of RES in rat plasma and various tissues. In addition, the method has been fully validated with good specificity, sensitivity, and precision. This method was successfully applied to study the bioavailability and tissue distribution of RES in rats. After a single intravenous administration of GL-HSA-RESNPs in rats, the bioavailability was 4.25 times higher than that of the same dose of raw RES. Moreover, the absorption rate of GL-HSA-RESNP in rats was faster than that of raw RES. This study established a method for the determination of RES by HPLC, which provides a reference value for evaluating the in vivo pharmacokinetics of RES in the future.

#### Disclosure statement

No potential conflict of interest was reported by the authors.

#### Funding

This work was supported by the Fundamental Research Funds for the Central Universities [2572018AA16] to M.W. and the Heilongjiang Touyan Innovation Team Program. C.Z. was sponsored by the Shanghai Talent Development funding.

#### References

Aihui MH, Tang Z, Hong W, et al. (2010). Protein-based nanomedicine platforms for drug delivery. *Small* 5:1706–21.

Bazzo KO, Souto AA, Lopes TG, et al. (2013). Evidence for the analgesic activity of resveratrol in acute models of nociception in mice. *J Nat Prod* 76:13–21.

Deng W, Qiu J, Wang S, et al. (2018). Development of biocompatible and VEGF-targeted paclitaxel nanodrugs on albumin and graphene oxide dual-carrier for photothermal-triggered drug delivery in vitro and in vivo. *Int J Nanomedicine* 13:439–53.

Ethemoglu MS, Seker FB, Akkaya H, et al. (2017). Anticonvulsant activity of resveratrol-loaded liposomes in vivo. *Neuroscience* 357:12–9.

Han L, Li J, Huang S, et al. (2011). Peptide-conjugated polyamidoamine dendrimer as a nanoscale tumor-targeted T1 magnetic resonance imaging contrast agent. *Biomaterials* 32:2989–98.

Hoonjan M, Sachdeva G, Chandra S, et al. (2018). Investigation of HSA as a biocompatible coating material for arsenic trioxide nanoparticles. *Nanoscale* 10:8031–41.

Hsu SC, Huang SM, Chen A, et al. (2014). Resveratrol increases anti-aging Klotho gene expression via the activating transcription factor 3/c-Jun complex-mediated signaling pathway. *Int J Biochem Cell Biol* 53: 361–71.

Jain S, Patel N, Lin S. (2015). Solubility and dissolution enhancement strategies: current understanding and recent trends. *Drug Dev Ind Pharm* 41:875.

Jiang T, Mo R, Bellotti A, et al. (2014). Drug delivery: gel-liposome-mediated co-delivery of anticancer membrane-associated proteins and small-molecule drugs for enhanced therapeutic efficacy. *Adv Funct Mater* 24:2258.

Kratz F. (2008). Albumin as a drug carrier: design of prodrugs, drug conjugates and nanoparticles. *J Control Release* 132:171–83.

Kumar S, Dilbaghi N, Rani R, et al. (2013). Novel approaches for enhancement of drug bioavailability. *Rev Adv Sci Engng* 2:133–54.

Kwok PC, Chan HK. (2014). Nanotechnology versus other techniques in improving drug dissolution. *Curr Pharm Des* 20:474–82.

Li H, Ke F, An Y, et al. (2013). Gemcitabine-loaded magnetic albumin nanospheres for cancer chemohyperthermia. *J Nanopart Res* 15:1513.

Li W, Ma J, Ma Q, et al. (2013). Resveratrol inhibits the epithelial-mesenchymal transition of pancreatic cancer cells via suppression of the PI-3K/Akt/NF-κB pathway. *Curr Med Chem* 20:4185–4194.

Li Z, Yang S, Chen T, Qiang X. (2005). Selective depletion of glycyrrhizin from Si-Ni-San, a traditional Chinese prescription, blocks its effect on contact sensitivity in mice and recovers adhesion and metalloproteinases production of T lymphocytes. *Int Immunopharmacol* 5: 1193–1204.

Liang L, Liu X, Wang Q, et al. (2013). Pharmacokinetics, tissue distribution and excretion study of resveratrol and its prodrug 3,5,4'-tri-O-acetyl-resveratrol in rats. *Phytomedicine* 20:558–63.

Liu Y, Tong L, Luo Y, et al. (2018). Resveratrol inhibits the proliferation and induces the apoptosis in ovarian cancer cells via inhibiting glycolysis and targeting AMPK/mTOR signaling pathway. *J Cell Biochem* 119:6162–72.

Merino S, Martín C, Kostarelos K, et al. (2015). Nanocomposite hydrogels: 3D polymer-nanoparticle synergies for on-demand drug delivery. *ACS Nano* 9:4686–97.

Mo Y, Barnett ME, Takemoto D, et al. (2007). Human serum albumin nanoparticles for efficient delivery of Cu, Zn superoxide dismutase gene. *Mol Vis* 13:746–57.

Moros M, Mitchell S, Grazu V, Fuente JM. d. (2013). The fate of nanocarriers as nanomedicines in vivo: important considerations and biological barriers to overcome. *Curr Med Chem* 20:2759–78.

Musthaba SM, Ahmad S, Ahuja A, et al. (2010). ChemInform abstract: Nano approaches to enhance pharmacokinetic and pharmacodynamic activity of plant origin drugs. *ChemInform* 41.

Sengupta P, Chatterjee B. (2017). Potential and future scope of nanoemulgel formulation for topical delivery of lipophilic drugs. *Int J Pharm* 526:353–65.

Singh A, Ahmad I, Ahmad S, et al. (2016). A novel monolithic controlled-delivery system of resveratrol for enhanced hepatoprotection: nanoformulation development, pharmacokinetics and pharmacodynamics. *Drug Dev Ind Pharm* 42:1524–36.

- Szkudelska K, Nogowski L, Szkudelski T. (2014). Adipocyte dysfunction in rats with streptozotocin-nicotinamide-induced diabetes. *Int J Exp Path* 95:86–94.
- Taneja N, Singh KK. (2017). Rational design of polysorbate 80 stabilized human serum albumin nanoparticles tailored for high drug loading and entrapment of irinotecan. *Int J Pharm* 536:82–94.
- Wang Z, Chen L, Chu Z, et al. (2018). Gemcitabine-loaded gold nanoparticles mediated by albumin for enhanced anti-tumor activity combining with CT imaging. *Mater Sci Eng C Mater Biol Appl* 89:106–18.
- Wang D, Xu Y, Liu W. (2008). Tissue distribution and excretion of resveratrol in rat after oral administration of *Polygonum cuspidatum* extract (PCE). *Phytomedicine* 15:859–66.
- Wang L, Zhang H, Qin A, et al. (2016). Theranostic hyaluronic acid pro-drug micelles with aggregation-induced emission characteristics for targeted drug delivery. *Sci China Chem* 59:1–7.
- Wu M, Lian B, Deng Y, et al. (2017). Resveratrol-loaded glycyrrhizic acid-conjugated human serum albumin nanoparticles wrapping resveratrol nanoparticles: preparation, characterization, and targeting effect on liver tumors. *J Biomater Appl* 32:191–205.
- Yin T, Zhang Q, Wu H, et al. (2017). In vivo high-efficiency targeted photodynamic therapy of ultra-small Fe<sub>3</sub>O<sub>4</sub>@polymer-NPO/PEG-Glc@Ce6 nanoprobe based on small size effect. *NPG Asia Mater* 9:e383–e383.
- Yu Z, Yu M, Zhou Z, et al. (2014). Novel flower-shaped albumin particles as controlled-release carriers for drugs to penetrate the round-window membrane. *Int J Nanomedicine* 9:3193–201.
- Zhu X, Wu C, Qiu S, et al. (2017). Effects of resveratrol on glucose control and insulin sensitivity in subjects with type 2 diabetes: systematic review and meta-analysis. *Nutr Metab (Lond)* 14:60.
- Zu Y, Zhang Y, Wang W, et al. (2016). Preparation and in vitro/in vivo evaluation of resveratrol-loaded carboxymethyl chitosan nanoparticles. *Drug Deliv* 23:971–91.